Alteration of gene conversion tract length and associated crossing over during plasmid gap repair in nuclease-deficient strains of *Saccharomyces cerevisiae*

Lorraine S. Symington*, Leslie E. Kang and Sylvie Moreau

Department of Microbiology and Institute of Cancer Research, Columbia University College of Physicians and Surgeons, 701 West 168th Street, New York, NY 10032, USA

ABSTRACT

A plasmid gap repair assay was used to assess the role of three known nucleases, Exo1, Mre11 and Rad1, in the processing of DNA ends and resolution of recombination intermediates during double-strand gap repair. In this assay, alterations in end processing or branch migration are reflected by the frequency of co-conversion of a chromosomal marker 200 bp from the gap. Gap repair associated with crossing over results in integration at the homologous chromosomal locus, whereas the plasmid remains episomal for non-crossover repair events. In *mre11* strains, the frequency of gap repair was reduced 3- to 10-fold and conversion tracts were shorter than in the wild-type strain, consistent with a role for this nuclease in processing double-strand breaks. However, conversion tracts were longer in a strain containing the nuclease deficient allele, *mre11-H125N*, suggesting increased end processing by redundant nucleases. The frequency of gap repair was reduced 2-fold in *rad1* mutants and crossing over was reduced, consistent with a role for Rad1 in cleaving recombination intermediates. The frequency of gap repair was increased in *exo1* mutants with a significant increase in crossing over. In *exo1 mre11* double mutants gap repair was reduced to below the *mre11* single mutant level.

INTRODUCTION

Deoxyribonucleases are involved in many aspects of DNA metabolism, including replication, repair and recombination. Models for the repair of DNA double-strand breaks (DSBs) by recombination invoke nuclease processing at multiple steps (1). Nucleases are predicted to resect the ends at DSBs to generate intermediates with 3′ single-stranded tails. This could occur by the activity of a double-stranded exonuclease, or a single-stranded endo- or exonuclease working in concert with a helicase. Intermediates with 3′ single-stranded tails have been identified during meiotic recombination and at the *MAT* locus during mating type switching (2,3). Following homologous pairing and strand invasion to produce heteroduplex DNA, the displaced strand (D-loop) may pair with the other side of the break to form an intermediate with Holliday junctions. The Holliday junctions can be resolved by branch migration or endonucleolytic cleavage (4). Alternatively, the D-loop formed by strand invasion could collapse after limited DNA synthesis to displace the invading 3′-end (5), resulting in gap repair without an associated crossover. Mismatches present in heteroduplex DNA are repaired by the mismatch repair system, which involves exonucleolytic processing of one strand of the heteroduplex to the site of the mismatch (6,7).

The nucleases involved in each of these steps in *Escherichia coli* have been identified by genetic and biochemical methods, however, much less is known of the nucleases with equivalent functions in eukaryotes. Of the genes required for ionizing radiation resistance in yeast, most function at a step subsequent to the processing of DNA ends. The exceptions are the *MRE11*, *RAD50* and *XRS2* genes, the products of which function as a complex to regulate the processing of DSBs *in vivo*. In these mutants there is a delay in the resection of DSBs generated by the HO endonuclease, but repair still occurs (8). The Mre11 protein has endonuclease and 3′→5′ exonuclease activities *in vitro* (9–12). However, point mutations that abolish the nuclease activity of Mre11 *in vitro* cause no apparent defect in the processing step *in vivo* in mitotic cells, although they are defective in processing DSBs produced during meiosis (9,11–13). Furthermore, as the polarity of the Mre11 exonuclease is opposite to that predicted for resection of DSBs, this has raised the issue of whether Mre11 functions directly in the processing of ends. An alternate hypothesis is that the Mre11/Rad50/Xrs2 (MRX) complex unwinds DNA ends for the Mre11 endonuclease to clip off the 5′ strands, and this nuclease activity is redundant with other nucleases in mitotic cells (12).

Exonuclease I was identified from fractionated extracts of *Schizosaccharomyces pombe* and *Saccharomyces cerevisiae* as a 5′→3′ double-stranded deoxyribonuclease (14,15). As the polarity of degradation was the same as shown for resection of DSBs *in vivo*, and the activity was induced 5-fold in meiotic extracts of *S.pombe*, it appeared to be a good candidate for the nuclease active in processing DSBs (14). However, *exo1* mutants are not sensitive to ionizing radiation, are proficient at mating type switching and have only weak defects in meiosis (16,17). Although spore viability is not dramatically reduced in *exo1* mutants, there is a significant decrease in intergenic

recombination and an increase in meiosis I non-disjunction (18–20). Exo1 interacts with Msh2 and *exo1* mutants have a mutator phenotype suggesting a role in mismatch repair (16,21). The role of Exo1 in mitotic recombination is complex: the mutants show a decrease in spontaneous mitotic recombination between direct repeats and an increase in homeologous recombination (17,22). The latter is thought to be due to anti-recombination between diverged sequences observed for many mismatch repair mutants (23).

Rad1 is an essential component of the nucleotide excision repair (NER) pathway and mutants show high sensitivity to UV light (24,25). Rad1 forms a heterodimer with Rad10 that exhibits structure-specific endonuclease activity *in vitro* (26,27). This nuclease cleaves at the junction between duplex and single-stranded DNA at the 5′ side of a UV photoproduct during NER. In addition to the essential role in NER, Rad1 is required for certain mitotic recombination events to trim recombination intermediates with 3′ heterologous tails and in the repair of loop heteroduplexes formed during meiotic recombination (28,29). *rad1* mutants also exhibit defects in mitotic conversion tract length, gene replacement and in plasmid integration (30,31). The Rad1 nuclease has been shown to cleave artificial Holliday junctions generated from oligonucleotides, but the cleavages are not symmetrical like those observed for other Holliday junction resolvases, such as RuvC (32,33). Although *rad1* mutants of *S.cerevisiae* are sporulation proficient, mutation of the *Drosophila melanogaster* homolog of *RAD1*, *mei-9*, causes a defect in meiotic crossing over (34,35). It is possible that the Rad1 nuclease is redundant with another Holliday junction resolvase in yeast, or that the endonuclease activity cleaves other types of branched intermediates formed during recombination.

We have used a plasmid gap repair assay to evaluate the role of these nucleases in mitotic recombination (36,37). A plasmid containing a double-strand break or gap within a region of the plasmid homologous to chromosomal sequences is efficiently repaired when introduced into yeast cells by transformation. Homology-dependent gap repair predominates in recombination proficient cells, but end-joining events can also occur (36,37). If the gapped plasmid contains no origin of replication, only repair events associated with crossing over to integrate the plasmid at the homologous chromosomal locus are recovered. However, if the gapped plasmid contains an origin of replication repair events unassociated with crossing over also occur. Heteroduplex DNA formed adjacent to the gap during plasmid gap repair can be monitored by co-conversion of markers flanking the plasmid-borne gap. Thus, plasmid gap repair provides a convenient system to measure conversion tract lengths and associated crossing over during double-strand gap repair. Here we show that several nucleases implicated in mitotic recombination have both quantitative and qualitative effects on plasmid gap repair.

MATERIALS AND METHODS

Yeast strains and plasmids

All strains are derivatives of W303-1A or W303-1B with the corrected *RAD5* allele and are listed in Table 1 (38,39). Strains LSY697 and LSY698 containing the *met17-sna* and *met17::ADE2* alleles, respectively, have been described previously (37). The *met17-sna* allele results from a single base pair insertion within the *Sna*BI site that creates a stop codon and destroys the *Sna*BI site. These strains were crossed to other W303 derivatives containing the *exo1::HIS3*, *mre11::LEU2*, *mre11-H125N* or *rad1::LEU2* mutations and the resulting diploids sporulated to generate haploid progeny of the desired genotype. The plasmid substrates for gap repair, pSB101 and pSB110, were described previously (37). Briefly, pSB101 contains the *URA3* and *MET17* genes and no origin of replication; pSB110 is identical except for insertion of an *ARSH4* element.

Table 1. Yeast strains

Strain	Relevant genotype[a]	Source
LSY697	*MAT**a** met17-sna ADE2*	(37)
LSY698	*MAT**a** met17::ADE2*	(37)
LSY870-2C	*MAT**a** met17-sna ADE2 mre11::LEU2*	This study
LSY871-5A	*MAT**a** met17::ADE2 mre11::LEU2*	This study
LSY889-2D	*MAT**a** met17-sna ADE2 mre11::LEU2 exo1::HIS3*	This study
LSY894-4C	MAT**a** *met17-sna ADE2 exo1::HIS3*	This study
LSY895-10A	*MATα met17-sna ADE2 rad1::LEU2*	This study
LSY918-1	*MATα met17-sna ADE2 mre11-H125N*	This study
LSY920-20A	*MAT**a** met17-sna ADE2 mre11::LEU2 rad1::LEU2*	This study
LSY927-1C	*MAT**a** met17::ADE2 exo1::HIS3*	This study
LSY928-9C	*MAT**a** met17::ADE2 rad1::LEU2*	This study

[a]All strains are derivatives of W303-1A or W303-1B (*leu2-3,112*, *trp1-1*, *can1-100*, *ura3-1*, *ade2-1*, *his3-11,15 RAD5*), only differences from this genotype are listed above.

Media and growth conditions

Rich medium (YEPD), synthetic medium (SC) and lead-containing plates were prepared as described previously (40,41). Cultures and plates were incubated at 30°C unless otherwise stated. Methods for yeast transformation and tetrad dissection were as described previously (40).

Plasmid gap repair assays

Plasmids to be used as substrates for gap repair were digested with *Bsp*EI and *Eco*NI, and the large DNA fragment gel purified. Transformation of yeast cells was by the lithium acetate method using 100 ng of gapped plasmid or 100 ng of uncut pSB110 (transformation efficiency control) in the presence of 50 μg of denatured salmon sperm carrier DNA. For the *mre11 rad1* and *mre11 exo1* double mutants, 300 ng of gapped pSB110 and 600 ng of gapped pSB101 were used. The amounts of DNA used for transformation were determined to be in the linear range. The transformation efficiency using gapped plasmids was improved by inclusion of a 20 min, 30°C incubation step in SOS (1 M sorbitol, 0.3% yeast extract, 0.6% bacto-peptone, 6.5 mM $CaCl_2$) medium following heat shock. The transformed cells were diluted and plated onto SC-Ura and SC-Ura-Met media and colonies counted after 3 days incubation at 30°C. The gap repair frequency was calculated as the number of Met⁺ Ura⁺ transformants per microgram of transformed gapped

plasmid divided by the number of Met$^+$ Ura$^+$ transformants per microgram of uncut pSB110. The gap repair assay was performed at least three times for each strain and the mean values are presented.

Analysis of gap repair products

Ura$^+$ transformants were picked from transformation plates and patched on SC-Ura plates. After 2 days of growth, the cells were replica plated to SC-Met and YEPD plates to score for the Met phenotype and to allow non-selective growth. After 2 days of growth on YEPD, the transformants were replica plated onto 5-FOA and Pb^{2+} plates to assess the mitotic stability phenotype. Confluent growth on 5-FOA indicated that the Ura$^+$ phenotype was unstable. Integration of the plasmid results in a direct repeat and a stable Ura$^+$ phenotype due to the low rate of excision of the plasmid from the chromosomal duplication. Met$^-$ cells are pigmented dark brown due to the accumulation of PbS when grown on plates containing Pb^{2+}. Transformants that grew on SC-Met, but were dark brown on Pb plates following non-selective growth, were scored as unstable Met$^+$. The data in Table 3 were pooled from three independent transformations of each strain with the exception of the *mre11 rad1* strain, for which two independent analyses were performed. Within each strain, there was little variation in the ratios of Met$^+$ to Met$^-$ and integrated to non-integrated between transformations. Significance was determined by chi-squared tests.

The efficiency of gene replacement was determined by transforming strains containing the *met17::ADE2* allele with a 2.5 kb *Spe*I fragment containing *MET17* derived from pSB101 and selecting Met$^+$ transformants. Correct replacement of the *met17::ADE2* allele results in a Met$^+$ Ade$^-$ phenotype; the rare Met$^+$ Ade$^+$ transformants were deducted from the total number of Met$^+$ to calculate recombination efficiencies. The number of Met$^+$ transformants was normalized to the transformation efficiency using uncut pSB110.

RESULTS

Plasmid gap repair assay

We previously described a gap repair assay based on a series of plasmids containing the selectable/counter-selectable marker, *URA3*, and the selectable, colony-color marker, *MET17* (37). A 238 bp double-strand gap was made within the plasmid *MET17* gene by digestion with *Bsp*EI and *Eco*NI endonucleases. The gapped plasmid DNA was introduced into host cells containing a nonsense mutation within the chromosomal *MET17* gene, *met17-sna*, by transformation. The efficiency of repair was determined from the number of Met$^+$ transformants relative to the transformation efficiency with an uncut replicating plasmid. We assume linear and circular molecules enter cells with equal efficiency and this ratio is not altered in any of the mutants tested. To determine the spectrum of repair events, Ura$^+$ transformants were selected and analyzed for the Met phenotype and also for the mitotic stability of the plasmid markers. Gap repair unassociated with crossing over results in a Ura$^+$ phenotype that is mitotically unstable (Ura^{+u}), whereas gap repair associated with crossing over (integration) generates a stable Ura$^+$ phenotype (Ura^{+s}). Although direct repeat recombination can result in excision of the plasmid, these events occur at much lower frequency than plasmid mis-segregation.
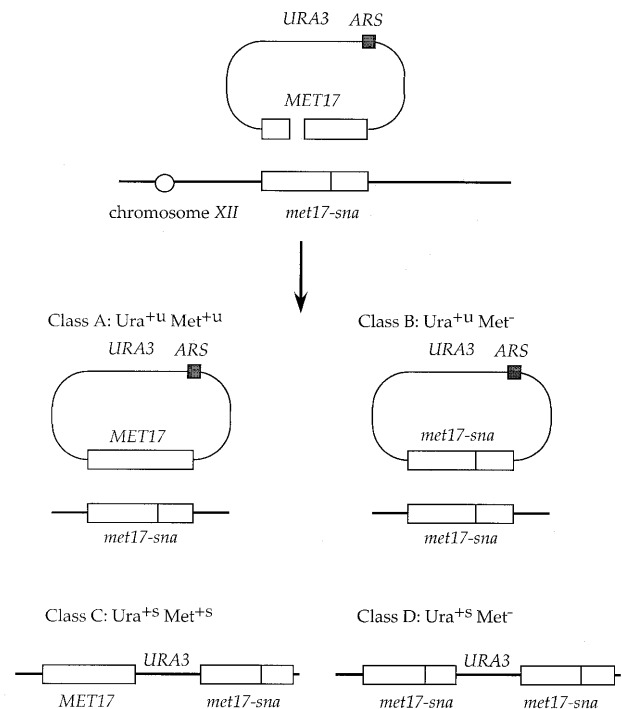

Figure 1. The gap repair assay. Repair of the gap within the *MET17* gene of pSB110 occurs by interaction with the homologous chromosomal locus. The chromosomal *met17-sna* mutation (elimination of the *Sna*BI site) is located 216 bp from the *Eco*NI site bordering the gap. Repair of the gap unassociated with crossing over generates an unstable Ura$^+$ (Ura^{+u}) phenotype, whereas repair associated with crossing over results in a stable Ura$^+$ (Ura^{+s}) phenotype. Co-conversion of the *met17-sna* mutation during gap repair results in a Met$^-$ phenotype, whereas repair events that do not extend to the *met17-sna* site, or heteroduplexes repaired in favor of the wild-type sequences, are Met$^+$. Repair of pSB101 can only occur by crossing over because the plasmid has no *ARS* element (yeast replication origin) for maintenance as an episome.

Four major classes of events were recovered from wild-type cells using the gapped *ARS*-containing plasmid (Fig. 1): Ura^{+u} Met^{+u}, Ura^{+u} Met$^-$, Ura^{+s} Met^{+s} and Ura^{+s} Met$^-$. Forty-nine percent of the Ura$^+$ transformants obtained from the wild-type strain were Met$^-$ and for both the integrated and episomal events the Met$^-$ phenotype was due to conversion of the plasmid *MET17* gene to *met17-sna* (37). Conversion from the chromosomal marker to the plasmid could occur by extension of the gap, or heteroduplex DNA (hDNA) formation adjacent to the gap, followed by mismatch repair (Fig. 2). For both HO-induced mitotic recombination and DSB-induced meiotic recombination the 3$'$-end at break sites remains intact and conversion events are thought to occur by mismatch correction of asymmetric hDNA (3,42). The frequency of conversion of a marker adjacent to the break or gap is distance-dependent and reflects the length of the 3$'$ single-stranded tail formed by resection of the 5$'$ strand (3). Although we assume the ratio of Met$^+$ to Met$^-$ transformants is directed by the length of the 3$'$ single-stranded tail, post-synaptic processing and mismatch repair could also influence co-conversion.

Table 2. Gap repair efficiency in *exo1*, *mre11* and *rad1* strains

Relevant genotype	Transformants /µg ×10^4 uncut pSB110	pSB110[a] gap repair (×10^{-2})[b]	Fold increase	pSB110[a] gap repair (×10^{-2})[b]	Fold increase	Gene replacement (×10^{-3})[c]	Fold increase
EXO1 MRE11 RAD1	17.6 ± 2.8	24.3 ± 7.4		4.4 ± 1.3		8.2 ± 1.6	
exo1Δ	16.2 ± 0.8	46.3 ± 9.6	1.9	9.8 ± 3.0	2.2	23.1 ± 2.9	2.8
mre11Δ	4.4 ± 1.8	7.4 ± 2.8	0.3	0.41 ± 0.1	0.09	21.9 ± 7.7	2.7
mre11-H125N	19.1 ± 6.5	18.4 ± 5.4	0.8	ND[d]		ND	
rad1Δ	13.2 ± 3.9	16.0 ± 5.0	0.7	1.9 ± 0.8	0.4	2.6 ± 1.1	0.3
exo1Δ mre11Δ	0.9 ± 0.6	2.8 ± 1.6	0.1	0.08	0.02	ND	
rad1Δ mre11Δ	3.3 ± 1.6	4.8 ± 1.6	0.2	0.26 ± 0.03	0.06	ND	

[a]pSB110 is *ARS*$^+$; pSB101 contains no *ARS* element.
[b]Gap repair frequencies were determined by the number of Ura$^+$ Met$^+$ transformants obtained from the gapped plasmid divided by the number of Ura$^+$ Met$^+$ transformants obtained from an equivalent amount of uncut pSB110 DNA.
[c]Gene replacement frequencies were determined by the number of Met$^+$ transformants obtained from the *MET17* fragment divided by the number of Met$^+$ transformants obtained from an equivalent amount of uncut pSB110 DNA.
[d]ND, not determined.

Decreased efficiency of gap repair and reduction in conversion tract length in the *mre11* mutant

The Mre11 nuclease is implicated in the end-processing step based on physical studies of DNA intermediates formed during DSB repair. We expected to see an increase in the ratio of Met$^+$ to Met$^-$ transformants in *mre11* mutants if the Mre11 nuclease in involved in the processing reaction. The efficiency of gap repair with gapped pSB110 was reduced 3-fold in the *mre11Δ* strain with a significant increase in the number of Met$^+$ transformants and a decrease in the number of integration events ($P < 0.001$) (Tables 2 and 3). The class of transfomants showing the greatest alteration in number was the Ura^{+u} Met^{+u} class, which represented 55% of the total Ura$^+$ transformants in the *mre11Δ* strain, compared with 40% in the wild-type strain (Table 3). To determine whether the nuclease activity of Mre11, or some other function of Mre11, is responsible for the alteration in the spectrum of recombination products, the gap repair assay was performed in an *mre11-H125N* strain, which contains a point mutation abolishing the Mre11 nuclease activity (12). The efficiency of gap repair was only slightly reduced compared with the wild-type strain and was significantly higher than the *mre11Δ* strain (Table 2). Surprisingly, the percentage of Ura$^+$ transformants that were Met$^+$ was much lower than the wild-type and *mre11Δ* strains ($P < 0.001$) (Table 3). The *mre11-H125N* strain was the only one examined in which the Ura^{+u} Met$^-$ class exceeded 50% of the total and the Ura^{+u} Met^{+u} class was <29% of the total. The *mre11Δ* strain showed a significant reduction in the number of integration events, suggesting that the defect in gap repair was likely to be enhanced using the non-replicating vector, pSB101. Ura$^+$ transformants derived from pSB101 are all stable and result from integration of the plasmid. There was a 10-fold decrease in gap repair efficiency of pSB101 in the *mre11Δ* strain, compared with wild-type, an even greater decrease than predicted.

Plasmid integration is reduced in *rad1* mutants

Mutation of the *RAD1* gene has previously been shown to cause severe defects in plasmid integration and one-step gene replacement (30). The frequency of gap repair of pSB110 was reduced less than 2-fold in the *rad1* strain (Table 2). However, there was a significant reduction in the number of integration events recovered ($P < 0.001$) (Table 3). As expected, based on the low frequency of integration of pSB110, there was a greater decrease in gap repair efficiency using the non-replicating gapped plasmid. Because there was a reduction in crossing over (integration) in both the *mre11* and *rad1* strains, a *rad1 mre11* mutant was also tested to see if these nucleases function in the same or different pathways. The effect of the two mutations on the frequency of gap repair was additive suggesting both nucleases contribute to efficient gap repair. Ura$^+$ transformants from the *mre11 rad1* strain showed the same ratio of Met$^+$:Met$^-$ as observed for the *mre11Δ* strain, and the same ratio of integrated to episomal events as the *rad1* strain.

Gap repair efficiency and integration are increased by mutation of *EXO1*

The efficiency of gap repair was increased by almost 2-fold in the *exo1* strain (Table 2) and analysis of the Ura$^+$ products revealed a significant increase in the number of integration events ($P < 0.001$) (Table 3). The ratio of Met$^+$:Met$^-$ events was not significantly different from the wild-type strain, suggesting that Exo1 does not normally affect the processing of DSBs. Strains deleted for both *MRE11* and *EXO1* show enhanced sensitivity to methyl methane sulfonate (MMS) and slower processing of an HO-induced DSB than *mre11* single mutants (20). To determine whether the Mre11 and Exo1 nucleases act independently in processing plasmid DSBs, the gap repair assay was repeated in an *exo1 mre11* double mutant. The efficiency of gap repair of pSB110 was reduced 19-fold compared with the *exo1* strain, 10-fold compared with wild-type and 3-fold compared with the *mre11* strain, consistent with the synergism observed in other DNA repair assays. Analysis of Ura$^+$ products

Table 3. Distribution of Ura[+] products from pSB110 gap repair

Relevant genotype	Total Ura[+a]	Met[+b]	Short tract non-crossover (Ura[+u] Met[+u])	Long tract non-crossover (Ura[+u] Met[-])	Short tract corssover (Ura[+s] Met[+s])	Long tract crossover (Ura[+s] Met[-])	Others[c]	% Crossovers
RAD1 EXO1 MRE11	926	50.9	40.3	36.4	9.5	12.6	1.2	22.1
mre11Δ	675	62.9[d]	55.4	29.3	7.6	7.7	0	15.3[d]
mre11-H125N	516	34.9[d]	28.1	52.3	6.8	12.6	0.2	19.4
rad1Δ	510	52.5	48.0	40.6	4.3	6.9	0.2	11.2[d]
mre11Δ rad1Δ	406	66.5[d]	61.1	26.1	5.4	7.4	0	12.8[d]
exo1Δ	415	54.9	37.6	28.9	17.1	16.1	0.2	33.2[d]
mre11Δ exo1Δ	477	65.0[d]	40.9	23.5	24.1	11.5	0	35.6[d]

[a]Number of Ura[+] transformants analyzed; the other numbers are given as percentages of the total Ura[+].
[b]Percentages of Ura[+] transformants that were Met[+].
[c]Percentages of transformants that were classified as Ura[+s] Met[+u] and Ura[+u] Met[+s].
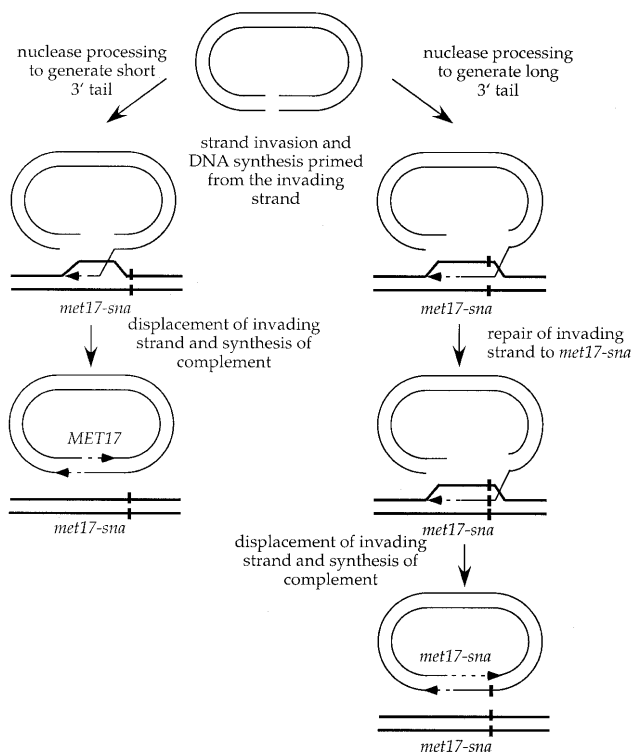[d]Significantly different from wild-type ($P < 0.001$).

Figure 2. Origin of the Met[+] and Met[-] recombinants. Extensive processing of the ends flanking the plasmid gap generates long 3′ single-stranded tails including the *MET17 Sna*BI site. Heteroduplexes resulting from strand invasion will contain the mutant and wild-type *Sna*BI sites. Mismatch repair of the invading strand will result in *met17-sna* information on the invading strand. Following DNA synthesis from the invading 3′-end, the invading strand is displaced and pairs with the 3′ tail at the other side of the break. DNA synthesis initiated from the other 3′-end, or by coupled lagging strand synthesis during the initial invasion, will duplicate the *met17-sna* allele. Less extensive processing of the break will result in the *MET17 Sna*BI site remaining double-stranded and it will not be incorporated into hDNA during strand invasion.

revealed the same distribution of Met[+]:Met[-] transformants as observed for the *mre11* strain and the high level of crossing over characteristic of the *exo1* strain. In this strain, 24% of the Ura[+] transformants were stable Met[+]. Although the gap repair efficiency of pSB110 was reduced 10-fold, one-third of the products contained integrated plasmids suggesting that gap repair of pSB101 might be reduced only 3-fold compared with pSB110. However, the gap repair efficiency of pSB101 was reduced 100-fold in the double mutant, compared with the *exo1* strain, 50-fold compared with wild-type and 5-fold compared with the *mre11* mutant. The recombination frequency of gapped pSB101 in the *exo1 mre11* strain may be even lower than presented in Table 2 because only one Met[+] Ura[+] colony was obtained from four independent transformations.

The frequency of gene replacement is elevated in *exo1* and *mre11* mutants

Plasmid gap repair is thought to be similar to the repair of chromosomal DSBs in the requirement for templated repair of the gap from a homologous donor duplex. In contrast, gene replacement could occur by assimilation of a single strand from the linear duplex, or by two independent end invasions involving both ends of the targeting fragment (43). Previous studies revealed no defect in gene replacement in *rad50* mutants, and a 50-fold decrease in *rad1* mutants (30,44). We measured the efficiency of replacement of the chromosomal *met17::ADE2* insertion allele by a 2.5 kb fragment containing the *MET17* gene. Each end of the targeting fragment has 600 bp of homology shared with the chromosomal locus and there are no heterologies present at the ends that could present barriers to efficient recombination. Correct gene replacement results in a Met[+] Ade[-] phenotype. The efficiency of targeting was increased almost 3-fold in the *exo1* and *mre11* strains and reduced 3-fold by the *rad1* mutation (Table 2).

DISCUSSION

We have used a plasmid gap repair assay to determine the efficiency of double-strand gap repair, as well as alterations in
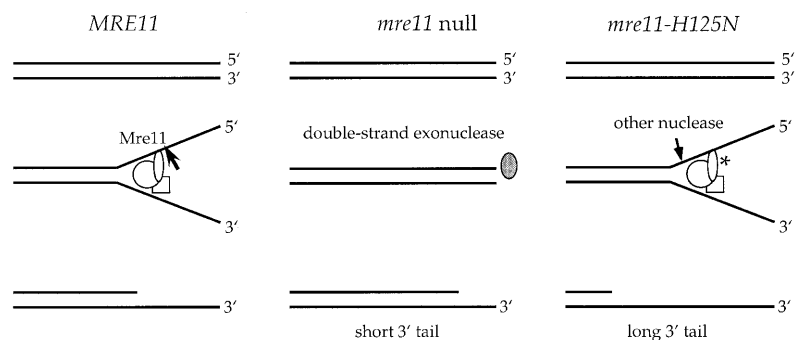
Figure 3. Models for end processing in *mre11* strains. In wild-type strains, the MRX complex binds to double-strand breaks and unwinds the ends producing single-stranded DNA, the substrate for the Mre11 endonuclease. In *mre11Δ* strains, the MRX complex is absent and no unwinding occurs, but the ends can be inefficiently processed by other exonucleases, such as Exo1. We imagine the MRX complex still forms in *mre11-H125N* strains and is able to unwind duplex ends, but the single-stranded tails are cleaved by other endo- or exonucleases. To account for apparent increase in gene conversion tract length, we propose that the redundant activities are more processive, or that unwinding by the MRX complex is normally coupled with the Mre11 endonuclease activity.

processing of recombination intermediates, in several nuclease-deficient strains of yeast. Most of the mutants examined were proficient at plasmid gap repair, but showed alterations in either conversion tract length or plasmid integration. These results are discussed in detail below.

Role of the Mre11 nuclease in end-processing events

Null mutations of *MRE11* cause severe defects in meiotic recombination and in survival to a variety of DNA damaging agents, including ionizing radiation, MMS and inter-strand crosslinking agents (45,46). Although the DNA repair defect is generally attributed to defective homologous recombination, *mre11Δ* mutants show elevated rates of spontaneous hetero-allelic recombination and only a small reduction in sister chromatid recombination (47). Kinetic studies of mating type switching revealed a reduction in the rate of resection of the 5′-end at HO-induced DSBs, and a delay in repair (48). Although Mre11 has endonuclease and exonuclease activity *in vitro*, mutations that abolish the nuclease activity do not alter the rate of resection of HO-induced DSBs (12). This suggests alternate roles for Mre11 (or the MRX complex) in regulation of the processing activity, or functional redundancy for the nuclease-processing step in mitotic cells. We found a 3-fold reduction in the efficiency of plasmid gap repair in *mre11Δ* mutants, but the *mre11-H125N* strain, defective for the nuclease function, showed almost wild-type levels of gap repair. In contrast, *rad52* and *rad51* mutants show 500- and 100-fold decreases, respectively, in the efficiency of gap repair (37,49). Therefore, the *mre11* deficiency in gap repair is much less severe than for other mutants of the *RAD52* epistasis group, but is consistent with studies of mating type switching and spontaneous mitotic recombination.

The altered ratio of Met⁺:Met⁻ events is consistent with decreased processing of the 5′-ends of break sites (Fig. 2). The *Sna*BI site is less likely to be incorporated into hDNA if the 3′ tails are shorter and, consequently, less likely to be co-converted with the gapped region. This alteration in the length of hDNA could possibly contribute to the hyper-recombination phenotype observed for heteroallelic recombination in *mre11* diploids. During heteroallelic recombination hDNA is likely to span

both alleles and co-repair of both mismatches would not generate a prototroph. However, if hDNA tracts are shorter so that only one of the two alleles is incorporated then prototrophs will be generated at higher frequencies. Surprisingly, repaired products were biased to Met⁻ from the strain containing the nuclease defective *mre11-H125N* allele (12). Our previous studies indicated no defect in mating type switching in this strain, but the physical analysis may not have detected an increase in the length of the 3′ single-stranded tails. We previously suggested redundancy for the nuclease-processing step in mitotic cells based on the weak DNA repair defects of the *mre11-H125N* strain. Based on the results presented here, we propose the MRX complex unwinds ends to provide access to the Mre11 endonuclease, or other nucleases that degrade single-stranded DNA (Fig. 3). In the absence of Mre11, the complex is absent and ends are processed inefficiently by a double-stranded DNA exonuclease, such as Exo1. In *mre11-H125N* strains, the ends are still unwound by the MRX complex, but are degraded by a more processive single-stranded DNA exonuclease or endonuclease, resulting in longer 3′ tails and increased co-conversion of the *Sna*BI site.

Previous studies of spontaneous mitotic recombination have found a correlation between conversion tract length and crossing over (50). We found a bias towards Met⁺ (short heteroduplex) among the non-crossover recombinants and a bias towards Met⁻ (long heteroduplex) among the crossover recombinants in the wild-type strains (Table 3). Therefore, the decrease in crossing over observed in *mre11Δ* strains could be a consequence of shorter heteroduplex tracts.

Rad1 influences crossing over during gap repair

The Rad1 endonuclease is reported to cleave artificial Holliday junctions generated from oligonucleotides (33). Although this result has been contested (51), the *rad1* mutation clearly affects plasmid integration, a process thought to occur by resolution of a Holliday junction intermediate. There are several possible explanations for this observation. First, as mentioned above, shorter heteroduplex tracts are associated with lower crossing over. This seems unlikely to be the cause of the integration defect in the *rad1* strain because co-conversion of
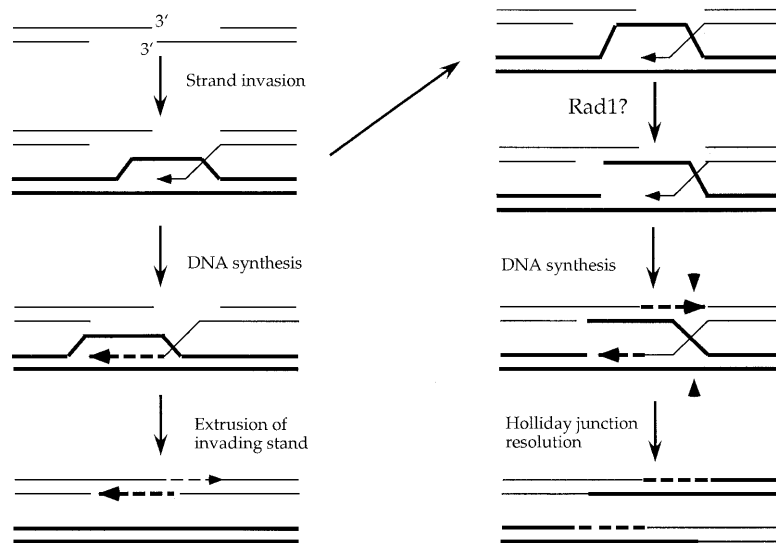
Figure 4. A model for Rad1 cleavage of recombination intermediates. Strand invasion occurs to form a D-loop structure and the invading 3′-end serves as a primer for DNA synthesis. If the elongated invading strand is extruded it can then pair with the single-strand extension at the other side of the break to repair the break with no associated crossover. Alternatively, the displaced strand of the unbroken duplex could pair with the single-strand tail on the other side of the break to form a double Holliday junction. We suggest Rad1 could cleave the D-loop structure to allow more efficient pairing or stabilization of the D-loop with the single-strand tail on the other side of the break. In the absence of Rad1 intermediates would be more likely to be channeled through the pathway on the left and thus less likely to be resolved as crossovers.

the *met17-sna* marker is the same as observed in the wild-type strain. Second, Rad1 could resolve some Holliday junction intermediates, especially if they contain single-stranded DNA near the junction. Third, Rad1 might cleave the D-loop formed by strand invasion (Fig. 4). This cleavage could possibly stabilize the intermediate by allowing pairing of the cleaved strand with the other side of the break to form a Holliday structure. The resulting double Holliday junction intermediate could then be resolved to form either crossover or non-crossover products. In the absence of Rad1, more intermediates would be resolved by D-loop collapse leading to fewer crossover events. Chiu *et al.* identified a structure-specific nuclease activity from *E.coli* extracts that stabilizes paranemic joints formed by recA (52); Rad1/10 could potentially act in a similar way to stabilize strand invasion intermediates made by Rad51. Finally, the D-loop could be cleaved by another endonuclease, and the tail subsequently removed by Rad1 to prevent competition for pairing with the invading strand.

Most of the previous studies demonstrating a defect in mitotic recombination in *rad1* mutants utilized substrates with heterologies at the site of a DSB that would require removal by the Rad1/10 endonuclease to complete the recombination event (28). In our studies of plasmid integration and gene replacement there are no heterologies present at the ends of the plasmid/fragment that might prevent efficient recombination. The defect in gene replacement observed in *rad1* mutants could be due to a requirement for Rad1 in processing the loop structure predicted to arise by single-strand assimilation, or by defective resolution of a strand invasion intermediate, as suggested above for plasmid gap repair.

exo1 mutants exhibit a hyper-recombination phenotype for gap repair and gene replacement

Strains deleted for *EXO1* have a complex phenotype indicative of defects in recombination and mismatch repair pathways (16,17,20–22). Although we detected no effect on end-processing events, the *exo1* strains showed a significant increase in both the frequency of gap repair and associated crossing over. Consistent with this observation, no alteration in heteroduplex tract length was observed at the *HIS4* locus during meiotic recombination (19). The increase in gap repair efficiency could be due to elimination of a degradative enzyme. However, this seems unlikely because we have not detected an increase in plasmid end joining in *exo1* strains (J.Ferguson and L.S.Symington, unpublished data) and a large excess of carrier DNA is used during transformation.

The substrates for gap repair are homologous except for a single base pair insertion to create the *met17-sna* allele, 200 bp from the gapped region. This may be sufficient to trigger anti-recombination by the mismatch repair system. A recent study showed elevated rates of spontaneous recombination between homologous sequences in *exo1* strains. Therefore, it seems likely that the increased levels of gap repair and gene replacement observed in the *exo1* strains are due to a defect in the mismatch repair system. The increase in plasmid integration may also be attributed to a defect in mismatch repair as several studies have documented increased crossing over in mismatch repair defective strains (53,54). During meiosis, intergenic recombination is reduced almost 2-fold in *exo1* homozygotes in contrast to the increase in crossing over observed for plasmid gap repair (18–20). Exo1 is induced during meiosis and may interact with other meiosis-specific proteins to form complexes with altered specificity for recombination intermediates (20).

The *exo1 mre11* double mutant has slow growth and the efficiency of transformation was reduced ~20-fold compared with the wild-type strain. The frequency of plasmid gap repair was reduced in the double mutant, consistent with studies showing an enhancement of the *mre11* mutant MMS sensitivity by an *exo1* mutation (20). Although physical studies at the *MAT* locus revealed a greater stability of the cut fragment in *exo1 mre11* strains, the ratio of Met$^+$:Met$^-$ transformants during gap repair was not significantly different from the *mre11* single mutant. Like the *exo1* strain, the *exo1 mre11* double mutant showed a significant increase in crossing over of the *ARS*-containing plasmid, even though conversion tracts were shorter. Because integration events were common with the *ARS*-containing plasmid, we expected to observe only a 3-fold reduction in the gap repair frequency using the integrating plasmid, compared with the *ARS*-containing plasmid. However, the frequency was much lower than expected. This was also found for the *mre11* single mutant. Based on this, we suggest the *ARS* element plays an important role during gap repair in *mre11* strains. It is possible that gap repair can occur by an alternate mechanism, such as break-induced replication from the two ends of the plasmid (55,56), and these events are dependent on close proximity of an *ARS* element.

ACKNOWLEDGEMENTS

REFERENCES

1. Szostak,J.W., Orr-Weaver,T.L., Rothstein,R.J. and Stahl,F.W. (1983) *Cell*, **33**, 25–35.
2. White,C.I. and Haber,J.E. (1990) *EMBO J.*, **9**, 663–673.
3. Sun,H., Treco,D. and Szostak,J.W. (1991) *Cell*, **64**, 1155–1161.
4. West,S.C. (1997) *Annu. Rev. Genet.*, **31**, 213–244.
5. Ferguson,D.O. and Holloman,W.K. (1996) *Proc. Natl Acad. Sci. USA*, **93**, 5419–5424.
6. Cooper,D.L., Lahue,R.S. and Modrich,P. (1993) *J. Biol. Chem.*, **268**, 11823–11829.
7. Kolodner,R.D. and Marsischky,G.T. (1999) *Curr. Opin. Genet. Dev.*, **9**, 89–96.
8. Ivanov,E.L., Sugawara,N., White,C.I., Fabre,F. and Haber,J.E. (1994) *Mol. Cell. Biol.*, **14**, 3414–3425.
9. Furuse,M., Nagase,Y., Tsubouchi,H., Murakami-Murofushi,K., Shibata,T. and Ohta,K. (1998) *EMBO J.*, **17**, 6412–6425.
10. Paull,T.T. and Gellert,M. (1998) *Mol. Cell.*, **1**, 969–979.
11. Usui,T., Ohta,T., Oshiumi,H., Tomizawa,J., Ogawa,H. and Ogawa,T. (1998) *Cell*, **95**, 705–716.
12. Moreau,S., Ferguson,J.R. and Symington,L.S. (1999) *Mol. Cell. Biol.*, **19**, 556–566.
13. Nairz,K. and Klein,F. (1997) *Genes Dev.*, **11**, 2272–2290.
14. Szankasi,P. and Smith,G.R. (1992) *J. Biol. Chem.*, **267**, 3014–3023.
15. Huang,K.N. and Symington,L.S. (1993) *Mol. Cell. Biol.*, **13**, 3125–3234.
16. Szankasi,P. and Smith,G.R. (1995) *Science*, **267**, 1166–1169.
17. Fiorentini,P., Huang,K.N., Tishkoff,D.X., Kolodner,R.D. and Symington,L.S. (1997) *Mol. Cell. Biol.*, **17**, 2764–2773.
18. Khazanehdari,K.A. and Borts,R.H. (2000) *Chromosoma*, **109**, 94–102.
19. Kirkpatrick,D., Ferguson,J., Petes,T.D. and Symington,L.S. (2000) *Genetics*, in press.
20. Tsubouchi,H. and Ogawa,H. (2000) *Mol. Biol. Cell*, **11**, 2221–2233.
21. Tishkoff,D.X., Boerger,A.L., Bertrand,P., Filosi,N., Gaida,G.M., Kane,M.F. and Kolodner,R.D. (1997) *Proc. Natl Acad. Sci. USA*, **94**, 7487–7492.
22. Nicholson,A., Hendrix,M., Jinks-Robertson,S. and Crouse,G.F. (2000) *Genetics*, **154**, 133–146.
23. Datta,A., Hendrix,M., Lipsitch,M. and Jinks-Robertson,S. (1997) *Proc. Natl Acad. Sci. USA*, **94**, 9757–9762.
24. Cox,B.S. and Parry,J.M. (1968) *Mutat. Res.*, **6**, 37–55.
25. Game,J.C. and Cox,B.S. (1971) *Mutat. Res.*, **12**, 328–331.
26. Bailly,V., Sommers,C.H., Sung,P., Prakash,L. and Prakash,S. (1992) *Proc. Natl Acad. Sci. USA*, **89**, 8273–8277.
27. Bardwell,A.J., Bardwell,L., Tomkinson,A.E. and Friedberg,E.C. (1994) *Science*, **265**, 2082–2085.
28. Fishman-Lobell,J. and Haber,J.E. (1992) *Science*, **258**, 480–484.
29. Kirkpatrick,D.T. and Petes,T.D. (1997) *Nature*, **387**, 929–931.
30. Schiestl,R.H. and Prakash,S. (1988) *Mol. Cell. Biol.*, **8**, 3619–3626.
31. Aguilera,A. and Klein,H.L. (1989) *Genetics*, **123**, 683–694.
32. Bennett,R.J., Dunderdale,H.J. and West,S.C. (1993) *Cell*, **74**, 1021–1031.
33. Habraken,Y., Sung,P., Prakash,L. and Prakash,S. (1994) *Nature*, **371**, 531–534.
34. Dowling,E.L., Maloney,D.H. and Fogel,S. (1985) *Genetics*, **109**, 283–302.
35. Sekelsky,J.J., McKim,K.S., Chin,G.M. and Hawley,R.S. (1995) *Genetics*, **141**, 619–627.
36. Orr-Weaver,T.L. and Szostak,J.W. (1983) *Proc. Natl Acad. Sci. USA*, **80**, 4417–4421.
37. Bartsch,S., Kang,L.E. and Symington,L.S. (2000) *Mol. Cell. Biol.*, **20**, 1194–1205.
38. Thomas,B.J. and Rothstein,R. (1989) *Genetics*, **123**, 725–738.
39. Fan,H.Y., Cheng,K.K. and Klein,H.L. (1996) *Genetics*, **142**, 749–759.
40. Sherman,F., Fink,G. and Hicks,J. (1986) *Methods in Yeast Genetics*. Cold Spring Harbor Laboratory Press, Cold Spring Harbor, NY.
41. Cost,G.J. and Boeke,J.D. (1996) *Yeast*, **12**, 939–941.
42. Haber,J.E., Ray,B.L., Kolb,J.M. and White,C.I. (1993) *Proc. Natl Acad. Sci. USA*, **90**, 3363–3367.
43. Leung,W., Malkova,A. and Haber,J.E. (1997) *Proc. Natl Acad. Sci. USA*, **94**, 6851–6856.
44. Schiestl,R.H., Zhu,J. and Petes,T.D. (1994) *Mol. Cell. Biol.*, **14**, 4493–4500.
45. Ajimura,M., Leem,S.H. and Ogawa,H. (1993) *Genetics*, **133**, 51–66.
46. McHugh,P.J., Sones,W.R. and Hartley,J.A. (2000) *Mol. Cell. Biol.*, **20**, 3425–3433.
47. Bressan,D.A., Baxter,B.K. and Petrini,J.H. (1999) *Mol. Cell. Biol.*, **19**, 7681–7687.
48. Tsubouchi,H. and Ogawa,H. (1998) *Mol. Cell. Biol.*, **18**, 260–268.
49. Orr-Weaver,T.L., Szostak,J.W. and Rothstein,R.J. (1981) *Proc. Natl Acad. Sci. USA*, **78**, 6354–6358.
50. Jinks-Robertson,S., Michelitch,M. and Ramcharan,S. (1993) *Mol. Cell. Biol.*, **13**, 3937–3950.
51. Davies,A.A., Friedberg,E.C., Tomkinson,A.E., Wood,R.D. and West,S.C. (1995) *J. Biol. Chem.*, **270**, 24638–24641.
52. Chiu,S.K., Low,K.B., Yuan,A. and Radding,C.M. (1997) *Proc. Natl Acad. Sci. USA*, **94**, 6079–6083.
53. Selva,E.M., New,L., Crouse,G.F. and Lahue,R.S. (1995) *Genetics*, **139**, 1175–1188.
54. Inbar,O., Liefshitz,B., Bitan,G. and Kupiec,M. (2000) *J. Biol. Chem.*, **275**, 30833–30838.
55. Malkova,A., Ivanov,E.L. and Haber,J.E. (1996) *Proc. Natl Acad. Sci. USA*, **93**, 7131–7136.
56. Morrow,D.M., Connelly,C. and Hieter,P. (1997) *Genetics*, **147**, 371–382.